IEEE Access
Multidisciplinary ⋮ Rapid Review ⋮ Open Access Journal

Received 9 April 2023, accepted 23 April 2023, date of publication 28 April 2023, date of current version 15 May 2023.

Digital Object Identifier 10.1109/ACCESS.2023.3271600

APPLIED RESEARCH

Optimal Design and Experimental Study of Piezoelectric Vibrator With Multi-Order Bending Mode and Multi-Operating Frequency

JIAN ZHANG AND XIAOZHU WANG
Liaoning Provincial Key Laboratory of Energy Storage and Utilization, Yingkou Institute of Technology, Liaoning, Yingkou 115014, China
Corresponding author: Xiaozhu Wang (330608566@qq.com)

This work was supported in part by the Liaoning Natural Science Foundation Joint Fund Project 2021-YKLH-07, in part by the Liaoning Provincial Department of Education Funding for Scientific Research under Grant L2020007, in part by the Liaoning Natural Science Foundation Joint Fund Project 2020-YKLH-28, in part by the Program for Excellent Talents of Science and Technology in the Yingkou Institute of Technology under Grant RC202003, and in part by the Foundation of Liaoning Provincial Key Laboratory of Energy Storage and Utilization under Grant CNNK202312.

ABSTRACT In order to realize the accurate quantitative feeding of small block materials, this paper conducts theoretical and experimental research on the ultrasonic material conveying device, uses the ANSYS finite element analysis software to design the structure of the ring conveying vibrator, and conducts numerical analysis on the bending vibration modes and their corresponding natural frequencies of the conveying vibrator in the range of 20 kHz – 50 kHz, The influence of the structural parameters of the vibrator on its natural frequency and vibration mode is discussed in detail, the structural dimensions of the vibrator are determined, and the B_{11}, B_{15} order bending modes and corresponding natural frequencies of the conveying vibrator are optimized. By redesigning the polarization zoning of the piezoelectric ceramic chips, a multi frequency design scheme with multiple bending modes for the same piezoelectric vibrator is realized. On the basis of theoretical analysis, an experimental prototype of a large ring piezoelectric ultrasonic material conveying device is designed and manufactured, and the bending mode and resonant frequency of the conveying vibrator are experimentally verified. The experimental results show that the actual frequency of the B_{11}, B_{15} order bending mode of the conveying vibrator has certain deviation from the results of finite element analysis, but the frequency difference between the two resonant frequencies under the same order bending mode is almost zero. Finally, the conveying performance of the conveying device is tested experimentally. The designed conveying vibrator has good conveying capacity under the B_{11}, B_{15} order bending working modes, and the conveying speed is adjustable within a certain range (140 mm/s-450 mm/s).

INDEX TERMS Ultrasonic material conveying device, piezoelectric drive, ring vibrator, multiple drive frequencies, conveying performance.

I. INTRODUCTION

With the continuous improvement of production automation, material conveying is an indispensable part of the automatic production line. Its conveying efficiency determines the merits of the entire automatic production line. Therefore, higher requirements are put forward for its structure, noise, working principle, conveying accuracy and control difficulty [1], [2]. The traditional vibration conveyor based on the principle of electromagnetic energy conversion is more and more difficult to meet the requirements of automatic processing, packaging, assembly and other production lines for light industry and electronic products due to the disadvantages of large noise, slow response, heavy structure and low delivery accuracy [3]. Compared with other types of conveying device, the ultrasonic material conveying device has the advantages of

The associate editor coordinating the review of this manuscript and approving it for publication was Hassen Ouakad.

simple structure, less energy consumption, stable and reliable working performance, high feeding rate, good versatility, easy adjustment of feeding speed and no electromagnetic interference. Moreover, the piezoelectric vibration feeding device in the ultrasonic frequency domain moves smoothly and orderly with high efficiency due to its silent vibration feeding carrier and small amplitude, It has a very broad application prospect in the production fields requiring low noise and clean environment such as drug delivery and electronic components [4], [5].

The piezoelectric vibrator of the traditional ultrasonic material conveying device can only realize one bending mode. Under the same driving conditions, the conveying performance of different materials is very different, and the range of conveying speed is very small, which cannot transport materials stably; therefore, it is necessary to continuously adjust the frequency of the power, the control mode of ultrasonic material conveying device is complicated. At the same time, considering that the working frequency of ultrasonic material conveying device is generally more than 20 kHz [6], special ultrasonic frequency domain power supply is required, which increases the cost of ultrasonic material conveying device.

In order to realize accurate and quantitative conveying of small volume bulk materials and solve the problem that traditional ultrasonic material conveying device can only run in one bending mode, the ultrasonic material conveying device with multiple working frequencies is designed in this paper, that is, the same piezoelectric conveying vibrator can run in different working modes. The ring piezoelectric vibrator is selected as the transducer of the ultrasonic material conveying experimental device. By redesigning the polarization zoning of the piezoelectric ceramic chips, the multi working frequency design scheme of the same piezoelectric vibrator with multiple bending modes is realized, which improves the conveying performance of the conveying device, and the purpose is to provide a test platform for the theoretical and experimental research of macroscopic conveying performance such as ultrasonic conveying speed.

II. STRUCTURE DESIGN AND PROTOTYPE MANUFACTURE OF PIEZOELECTRIC VIBRATOR WITH DRIVING TEETH

The performance of ultrasonic material conveying device mainly depends on the vibration characteristics of the vibrator, which mainly includes the design of vibration mode, the selection of internal and external diameters, the design of vibrator thickness, the design of teeth, and the selection of ceramic chips [7], [8]. Modal analysis is an effectively tool to optimize the design of the vibrator. Through the vibration modal analysis of the vibrator, the structural size of the vibrator is constantly modified, so as to find the required vibration mode and corresponding resonant frequency [9].

A. STRUCTURE DESIGN OF VIBRATOR

As the driving power of the conveying device, piezoelectric vibrator is the core part of the ultrasonic material conveying device, which is composed of piezoelectric materials and elastomers. Elastic materials have a great impact on the conveying performance [10]. The selection is made according to the requirements of the life, efficiency, and cost, application environment of the conveying device, while taking into account the internal loss, processing performance, expansion coefficient, cost and other factors of the material. The vibrator structure is shown in Figure 1.

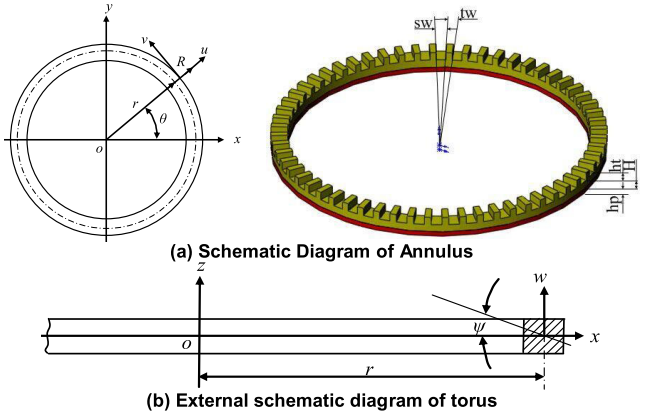

FIGURE 1. Structure of the piezoelectric vibrator.

When the ring conveying vibrator is used to transport materials, the running track of materials is a circular arc, and centrifugal force and other factors have adverse effects on material transport. Therefore, the large ring piezoelectric vibrator is used to improve the effect of curvature on material transport performance by increasing the arc radius [10].

The tooth structure is evenly distributed on the vibrator ring. These protruding teeth can increase the equivalent thickness of the vibrator without increasing the bending stiffness and natural frequency of the vibrator, so as to amplify the amplitude of the vibrator in bending vibration, so as to better promote the movement of materials. In addition, since the conveying device uses the tangential friction between the piezoelectric vibrator and the material to push the material forward, the friction between the two will produce a small amount of debris, which will constantly fall into the slot of the vibrator to ensure the normal operation of the conveying device.

When the ring piezoelectric vibrator performs out of plane bending vibration, the frequency difference between two bending modes of the same order is theoretically zero, which provides design convenience for the superposition of two bending standing waves of the same frequency into a bending traveling wave [11], [12]. Assume that the ring surface of the vibrator is of equal section and the section size is much smaller than the radius of the ring centerline, while the ring section remains flat during vibration. Select cylindrical coordinate system $R\ \theta\ Z$, analyzes the vibration of the ring, and assumes that the displacement of any point on the axis (section centerline) is u, v, w, and the rotation angle around the axis is ψ, if high-order trace is omitted, and then the

natural frequencies 'f_n' of each order is [11]

$$f_n = \frac{1}{2\pi r^2}\sqrt{\frac{EI_r}{\rho A}\cdot\frac{n^2(n^2-1)^2}{n^2+1+\mu}} \tag{1}$$

where, r is radius of the ring centerline, E is Elastic modulus, I_r is inertia moment of the section radius, ρ is the density, A is the cross-sectional area, n is the order of circumferential vibration mode, and μ is Poisson's ratio.

If the radius of outer ring is R_o, the radius of inner ring is R_i, and the height of ring is h, then the radius of ring center line (the equivalent radius of the vibrator ring) $r = (R_o + R_i)/2$, $I_r = (R_o\text{-}R_i)\ h3/12$, $A = (R_o\text{-}R_i)\ h$, taking the above parameters into equation (1), it can get [12]

$$f_n = \frac{2h}{\pi(R_o+R_i)^2}\sqrt{\frac{E}{12\rho}\cdot\frac{n^2(n^2-1)^2}{n^2+1+\mu}} \tag{2}$$

It is seen that when the width of the ring is fixed, the natural frequency of the ring is proportional to its height.

B. SELECTION OF VIBRATION MODE

Figure 2 shows the fifth order outside bending vibration mode diagram of the toothless torus under free boundary conditions. In Figure 2, (a) is the schematic diagram of the bending vibration mode of the outside ring; (b) is the ring bending modal diagram; (c) is the corresponding circular displacement mode cloud diagram. In the $B_{m,n}$ The number of pitch circles is m, and the number of pitch diameters is n. The ring piezoelectric vibrator of ultrasonic material conveying device driven by piezoelectric ceramic two-phase is designed in this paper, and the $B_{0,n}$ mode without pitch circle along the circumference is selected. So $m = 0$, the following modes are abbreviated as B_n.

By observing the bending mode with pitch circle in Figure 2, it is found that the amplitude of particle vibration at the pitch circle position is zero. The more pitch circles, the more particles with zero amplitude on the vibrator surface. Therefore, the existence of pitch circle is extremely unfavorable to the improvement of the conveying performance of the conveyor.

A kind of ultrasonic material conveying device with multiple working frequencies is designed in this paper, the same piezoelectric conveying vibrator can work in different working modes. In order to detect the conveying performance of the conveying device under different working frequencies, the natural frequency of the ring conveying vibrator should not be too high or too low during the mode selection, so as to prevent the driving force from weakening due to too small amplitude or too few driving points [13], [14]; At the same time, a certain frequency difference shall be ensured between the natural frequencies corresponding to different working modes of the same conveying vibrator [15].

Under the same excitation conditions, the larger the n is, the larger the resonant frequency of the vibrator is, the smaller the vibration amplitude of the vibrator is, and the output performance of the conveying device will be reduced. Therefore,

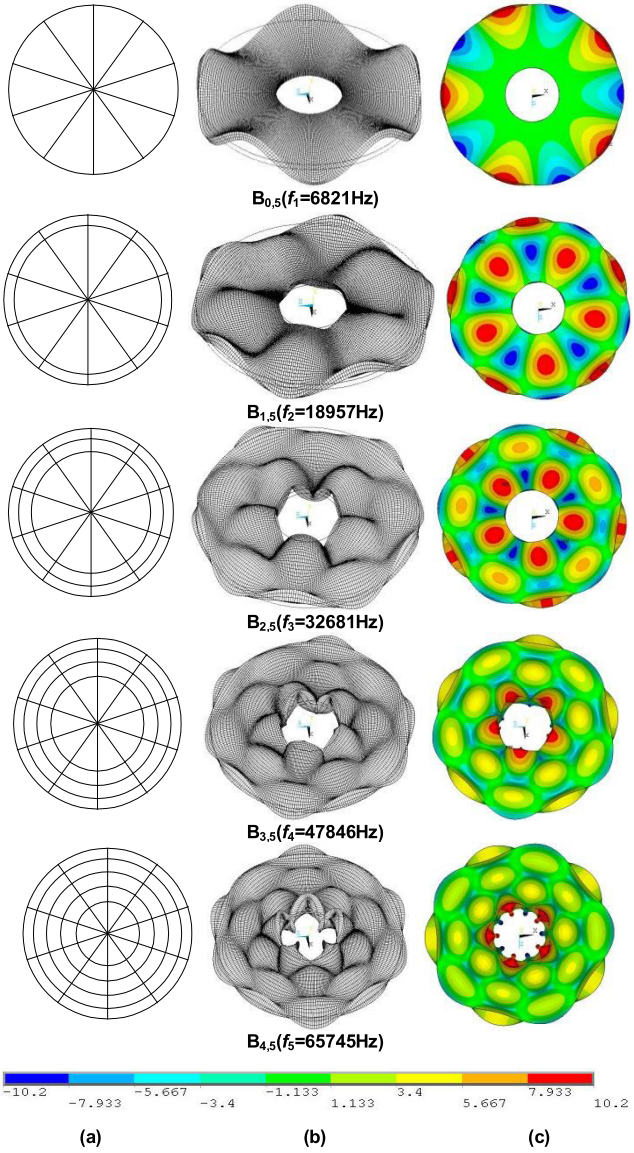

FIGURE 2. The out-plane bending vibration modes of the circular ring.

when the resonant frequency is fixed, the drive voltage must be increased to improve the transmission performance of the conveying device. However, the increase of the drive voltage increases the dielectric loss of the piezoelectric ceramics, increases the heating of the piezoelectric vibrator, and even causes the piezoelectric ceramics to crack. At the same time, high voltage and high frequency also bring great difficulties to the design and manufacture of the drive power. the smaller the n is, the smaller the resonant frequency of the vibrator is. Although the vibration amplitude has increased, the utilization rate of piezoelectric ceramics is low, which is not conducive to the improvement of the conveying performance of the conveying device. In addition, if the resonant frequency is lower than 20 kHz, it is easy to generate noise. Therefore, selecting the appropriate n can not only increase the vibration amplitude of the transport vibrator, but also facilitate the

design of the drive power. In this paper, the working modes of piezoelectric vibrator are selected as B_{11}, B_{15}.

C. FINITE ELEMENT ANALYSIS BASED ON ANSYS

Since the vibration amplitude of piezoelectric ceramics is very small by using the converse piezoelectric effect, the resonance of the vibrator must be used to amplify the amplitude, so it is very important to accurately calculate the natural frequency of the vibrator and the influence of various parameters on the natural frequency of the vibrator [16]. In this paper, ANSYS finite element analysis software is used to carry out numerical analysis and structural optimization of the outside bending mode of the vibrator.

Piezoelectric ceramic sheet is a key component of material conveying device, and its performance requirements are very high. Piezoelectric ceramic materials are required to have high mechanical quality factor, small dielectric loss, high power density and high mechanical strength, and have large electromechanical coupling coefficient and piezoelectric constant, as well as time and temperature stability. At present, the ultrasonic motor and ultrasonic material conveying device mainly use high-power piezoelectric ceramic materials. In this paper, PZT-81 ceramic is selected and polarized in the +Z direction.

D. DYNAMIC DESIGN OF VIBRATOR

Piezoelectric vibrator is composed of a ring elastic vibrator with convex teeth and a piezoelectric ceramic ring stuck at its bottom. In the analysis, the influence of the bonding layer between the vibrator's metal ring and the piezoelectric ceramic sheet is ignored [17], and the piezoelectric vibrator is regarded as a consolidated body with different materials. The influence of different structural parameters on the dynamic characteristics of the vibrator is analyzed by changing the parameters such as r/R (the ratio of inner radius to outer radius), H (the thickness of the vibrator), h_t (the tooth height), h_p (and the thickness of the piezoelectric ceramic chips), the tooth width.

1) INFLUENCE OF RING SIZE ON VIBRATOR MODAL

The shape of vibrator ring is determined by the outer radius R, inner radius r and thickness H. Firstly, the influence of r/R(the ratio of inner radius to outer radius) on the mode of the vibrator is analyzed. Under the condition that other dimensions remain unchanged, R is taken as 50 mm, the value range of r/R is 0.7 - 0.9, and the step size is 0.02. The change curve of the vibrator's natural frequency is shown in Figure 3. When r/R changes from 0.7 - 0.9, the ring width decreases gradually, and the natural frequency of the vibrator decreases significantly.

Figure 4 shows the change curve of the vibrator's natural frequency with the thickness of the vibrator. With the other dimensions of the vibrator unchanged, the thickness H of the vibrator changes between 1.5 mm and 4.5 mm, and the

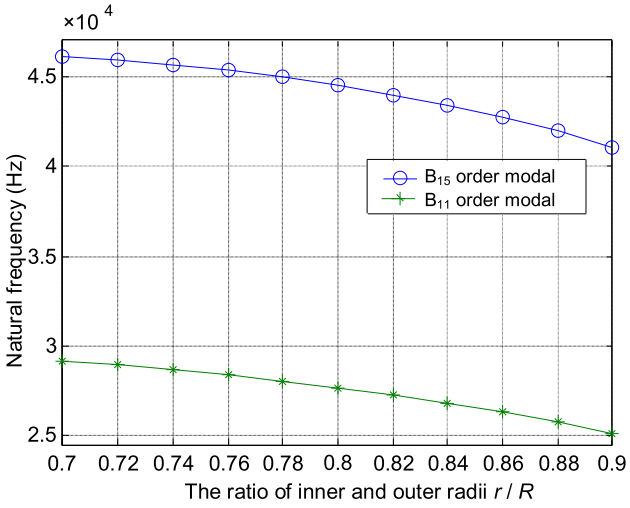

FIGURE 3. Influence of r/R on the natural frequencies.

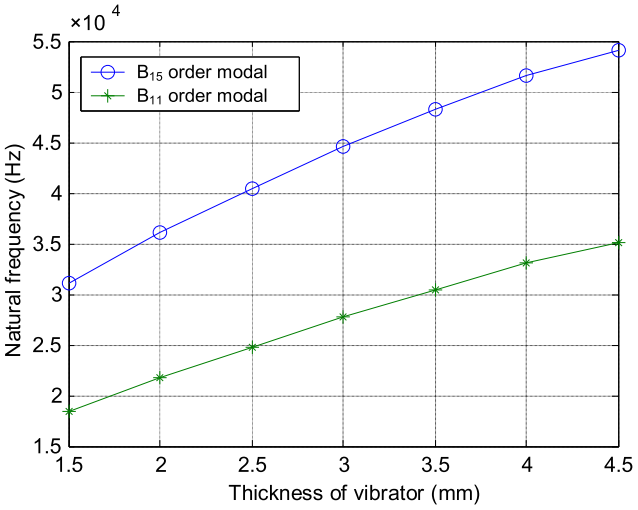

FIGURE 4. Influence of vibrator's thickness on the natural frequencies.

adjustment step is 0.5 mm. With the increase of the thickness of the vibrator, the natural frequency of the bending mode at the same order also increases, because the greater the thickness of the vibrator ring, the smaller the height of the convex teeth relative to the vibrator, and the smaller the impact on the vibration mode.

2) INFLUENCE OF VIBRATOR TOOTH ON MODE

Figure 5 shows the curve of natural frequency changing with tooth height. The variation range of tooth height is 1.5 mm - 4.5 mm, the increment is 0.5 mm. Other structural parameters remain unchanged. With the increase of the tooth, the natural frequency of the same order bending mode decreases. When the thickness of the vibrator's elastomer is fixed, the tooth will be bent if it is too high.

Figure 6 shows the curve of the natural frequency changing with the number of teeth. The range of the number of teeth

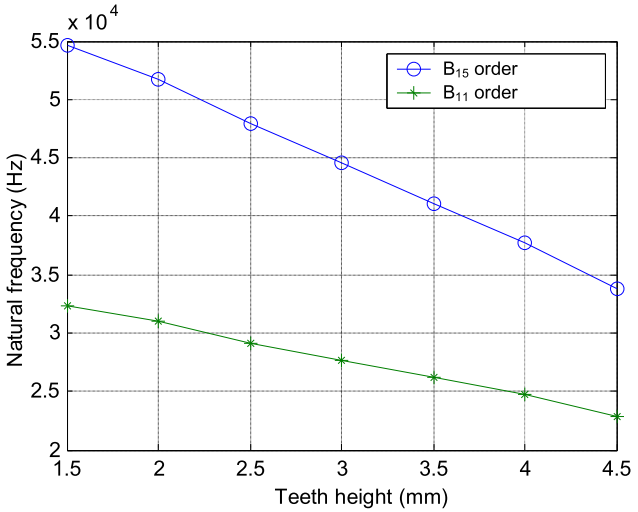

FIGURE 5. Influence of teeth height on the natural frequencies.

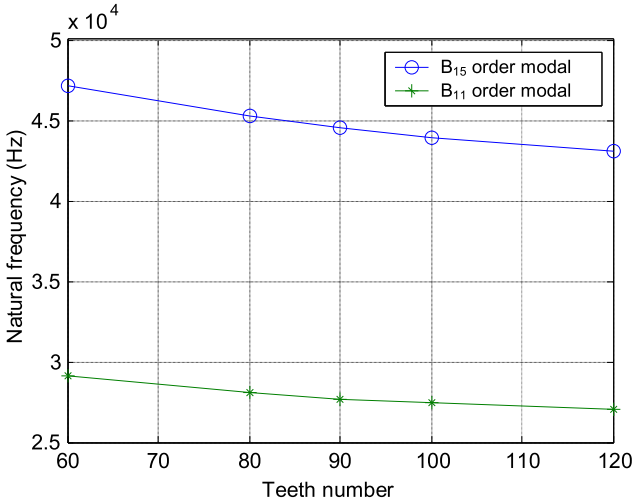

FIGURE 6. Influence of teeth number on the natural frequencies.

is 60 - 120 and the increment is 10. Under the condition that other parameters remain unchanged, the slot width of the vibrator is fixed at 0.4 mm (the center angle is 0.51°). Since the number of teeth and the width of the vibrator's the teeth are interrelated, the change of the tooth width is equivalent to the change of the convex teeth number, and the natural frequency of the vibrator decreases with the increase of the teeth number.

3) INFLUENCE OF CERAMIC THICKNESS ON MODAL

Figure 7 shows the change curve of natural frequency with ceramic thickness.

The other dimension parameters of the vibrator remain unchanged. The thickness of the ceramic chips varies from 0.5 mm to 1.5 mm, with a step of 0.1 mm. The natural frequency increases with the increase of the ceramic chips thickness, basically in a linear relationship.

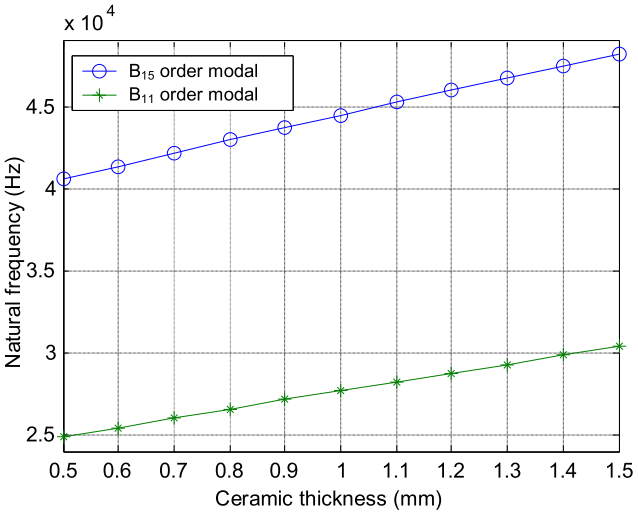

FIGURE 7. Influence of ceramic thickness on the natural frequencies.

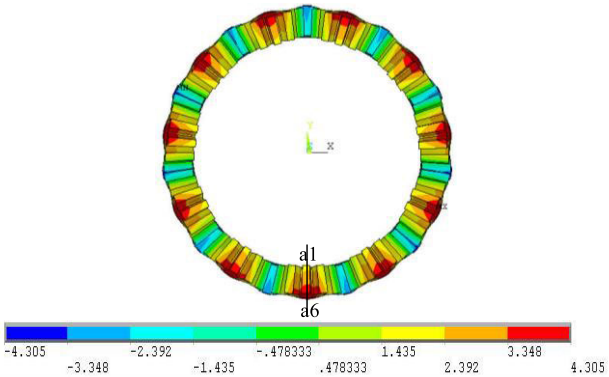

FIGURE 8. The displacement shape in Z direction of the vibrator.

4) SELECT THE STRUCTURAL SIZE OF THE VIBRATOR

Through the above analysis, the bending modes of the vibrator under different size parameters are simulated by using ANSYS finite element software. In order to facilitate the use of finite element software to model the vibrator, the convex tooth structure on the surface of the vibrator is generally positioned according to the degree, and the obtained tooth groove is a sector structure. Finally, the size of the vibrator structure is determined as follows: the width of the convex tooth on the vibrator's surface is 3.49°, the corresponding arc length of the outer ring is 3.0456 mm, and the arc length of the inner diameter is 2.4361 mm; The width of the tooth groove is 0.51°, the arc length of the corresponding outer ring is 0.4451 mm, the arc length of the inner diameter is 0.3560 mm, and the average tooth width is 0.4 mm.

E. RADIAL AMPLITUDE DISTRIBUTION OF PARTICLE ON THE SURFACE OF VIBRATOR

With the axis of the ring vibrator as the z-axis, the cylindrical coordinate system is established on the ring surface under the vibrator [18]. When sinusoidal and cosine voltages are

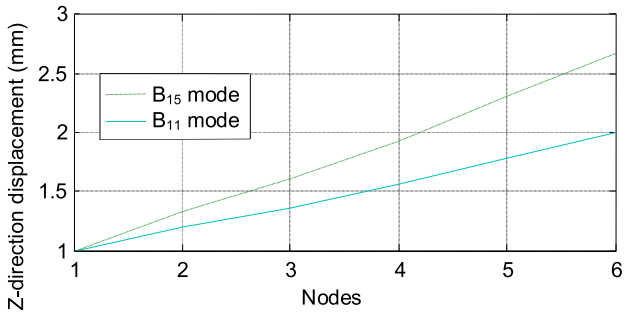

FIGURE 9. The amplitude distribution of the nodes on the wave crest.

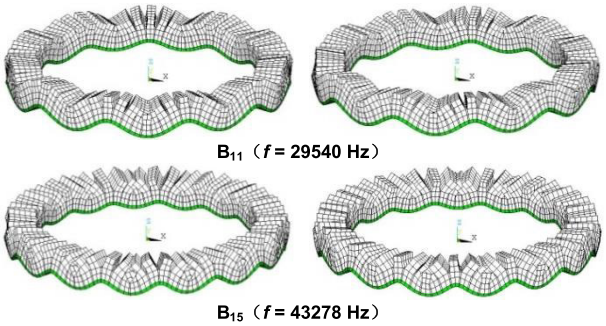

FIGURE 11. Bending vibration of the vibrators.

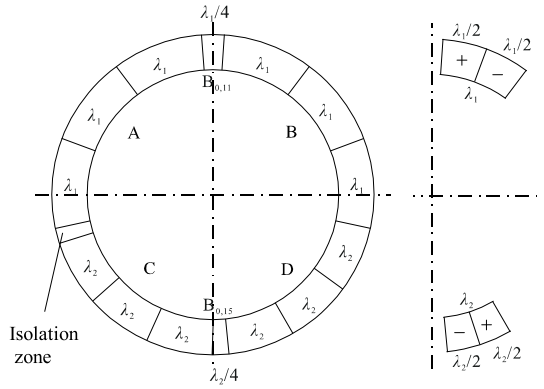

(a) Polarization mode of whole piezoelectric ceramic chips
(b) Polarization mode of ceramic chips within one wavelength

FIGURE 10. Polarization Zoning of Ceramic Sheet.

applied to the piezoelectric ceramics, the trajectory expression of any particle on the ring vibrator.

$$S_Z = S_1 + S_2 = AJ_m(kr)\cos(m\theta - \omega t) \tag{3}$$

where, S_Z is the synthesis of the motion track of any particle on the ring vibrator when the sine and cosine two-phase voltage are applied to the piezoelectric ceramic chips; S_1 is the motion track of any particle on the ring vibrator when a cosine phase voltage is applied to the piezoelectric ceramic chips; S_2 is the motion track of any particle on the ring vibrator when a sinusoidal phase voltage is applied to the piezoelectric ceramic chips; A is the cross-sectional area; $k = 2\pi/\lambda$ is the wave number of elastic wave vibration. J_{m} is the m-th order Bessel function; m is wave number; ω Angular frequency; r is the polar coordinate of the particle.

As can be seen from Eq. (3), at any time, the direction of traveling wave propagation θ and the radial coordinate r determines the amplitude of the vibrator particle. And the amplitude of the particle at $r = 0$ is zero, the amplitude of particle of identical θ coordinate increases with the increase of polar diameter coordinate r

Figure 8 is the Z-direction displacement mode diagram of the B_{11} order vibrator's bending mode. Select the nodes at the peak position of bending mode as the analysis object, and extract the Z-direction displacement of the node (6 nodes on each wave crest). As shown in Figure 8, the Z-direction amplitudes of nodes from inside to outside are a1, a2, a3, a4, a5 and a6 respectively.

In order to facilitate the comparison of amplitude distribution rules in Z direction of the vibrator under different bending modes, and avoid the change of amplitude values under different amplification conditions, if a1=1, the amplitude values from the inside to the outside nodes will change to: 1, a2/a1, a3/a1, a4/a1, a5/a1, and a6/a1. The amplitude distribution is shown in Figure 9.

It can be seen from Figure 9 that on the same radius, the Z-direction displacement of the node nearest to the circle center is the smallest, and the farther away from the center of the circle, that is, the larger the radius r, the greater the Z-direction displacement of the node, which is the same as the theoretical analysis of the radial amplitude distribution of the ring piezoelectric vibrator "The amplitude of particle of identical θ coordinate increases with the increase of polar diameter coordinate r".

F. PARTIAL POLARIZATION OF PIEZOELECTRIC CERAMICS

In the traditional zonal polarization mode of ring piezoelectric ceramic chips, the same frequency and equal amplitude alternating voltage with phase difference of $\pi/2$ between two phases is applied to the A and B regions of the piezoelectric ceramic chips respectively, which can excite the n-order traveling wave bending vibration of the piezoelectric vibrator. In this single zone polarization mode, the piezoelectric transport vibrator can only transport materials at one running frequency [19].

In order to investigate the influence of different vibration frequencies on the conveying speed and other characteristics of the ultrasonic material conveying device in a wide range, this paper rearranges the polarization zoning mode of the ring piezoelectric ceramic chips, and theoretically analyzes the different zoning polarization modes of piezoelectric ceramic chips of different sizes, as shown in Figure 10.

As shown in Figure 10, the bending mode of order B_{11} corresponds to the partition of the ceramic chip is $(6+1/4)\lambda_1$, about 204.55°, accounting for 56.82 % of the total ceramic ring, its wavelength λ_1 is the arc length corresponding to the 32.73° center angle on the circumference (the outer ring arc

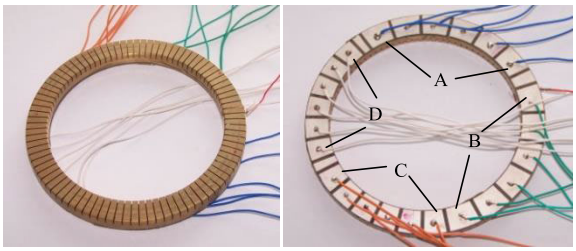

FIGURE 12. Physical structure diagram of ring vibrator.

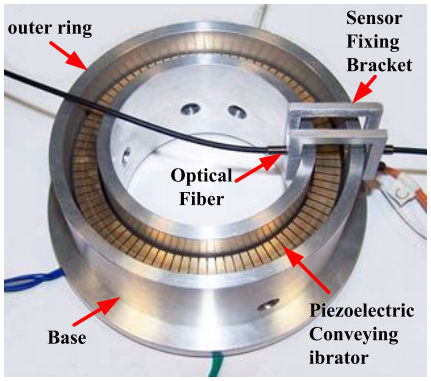

FIGURE 13. The prototype of the feeding device.

length is 28.56 mm, the inner ring arc length is 22.85 mm), Wavelength of 6 ceramic sector chips in zone A and B is λ_1, and about $\lambda_1/4$ is symmetrical; the bending mode of order B_{15} corresponds to the partition of the ceramic chip is $(6+1/4)\lambda_2$, about 150°, accounting for 41.67 % of the total ceramic ring, its wavelength λ_2 is the arc length corresponding to the 24° center angle on the circumference (the outer ring arc length is 28.56 mm, the inner ring arc length is 22.85 mm), Wavelength of 6 ceramic sector chips in zone C and D is λ_2, and about $\lambda_2/4$ is symmetrical; After zoning as shown in Figure 9, there is a 5.60° isolation area on the ring piezoelectric ceramic chip, which is connected with $\lambda_1/4$ $\lambda_2/4$ of the corresponding spacing area is used as the elastic support area of the piezoelectric vibrator.

According to the calculation of ANSYS finite element analysis software, the working frequencies of the B_{11}, B_{15} orders piezoelectric conveying vibrator are 29540 Hz and 43278 Hz, and their bending modes are shown in Figure 11.

G. MATERIAL SELECTION AND FABRICATION OF CERAMIC CHIP

Considering the dielectric constant, electromechanical coupling coefficient, piezoelectric constant, mechanical quality factor, and other performance parameters of piezoelectric materials, according to the results of structural design and modal analysis, the PZT-81 type piezoelectric ceramics were selected as the vibrator. The specifications are as follows: φ 100 mm $\times\varphi$ 80 mm $\times$ 1 mm, in the shape of a thin circle. as shown in Figure 12.

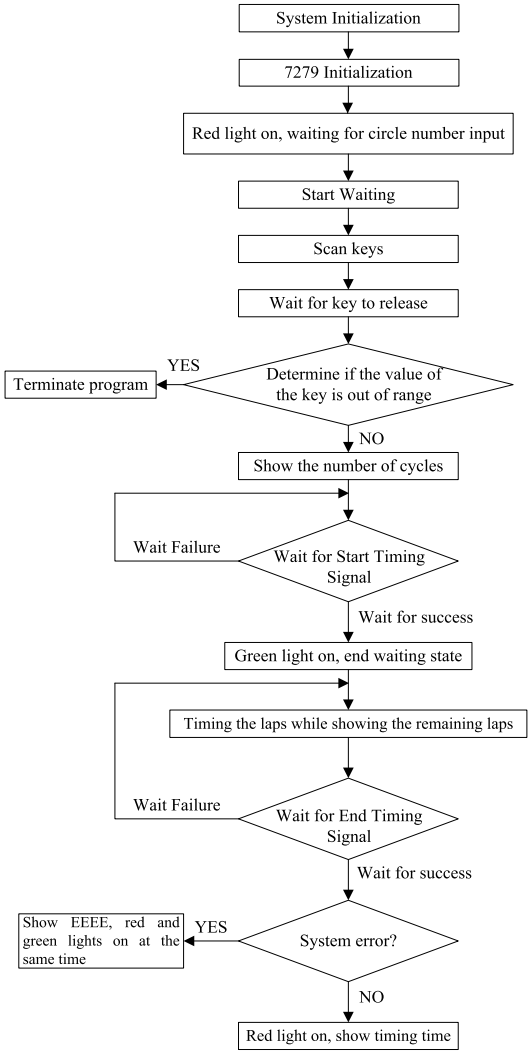

FIGURE 14. The main program flow chart.

III. THE DESIGN OF CONVEYING PERFORMANCE TESTING SYSTEM

Through the theoretical analysis of the vibrator's working principle, the structure of the vibrator is optimized by using the finite element analysis software, the structure and vibration mode of the vibrator were determined, and the experimental prototype of the ultrasonic material conveying device was designed and made, as shown in Figure 13.

The prototype is mainly composed of the following parts: piezoelectric conveying vibrator, base, outer ring, support part, bracket for fixing sensor and other experimental equipment. In order to meet the needs of the conveyor performance test, the set of single-chip timing system is designed in this paper. Figure 14 shows the flow chart of the single-chip timing system. As a whole machine design, it is required to strictly limit the machining accuracy of each part, such as surface roughness, symmetry, to ensure the appearance and installation accuracy. The vibration mode and conveying performance of the experimental prototype are tested. Based on the test results, the influence of driving voltage, running

TABLE 1. Resonant frequencies of the vibrator (unit: kHz).

Number of ceramic chips	A	B	C	D
Natural frequency of ANSYS modal analysis	27.679	27.679	44.519	44.519
Test the resonance frequency before installation	24.620	24.630	39.220	39.230
Test the resonant frequency after installation	24.690	24.690	39.310	39.310
working frequency	24.690	24.690	39.310	39.310

frequency and amplitude on the conveying speed is analyzed and discussed.

A. MODAL TEST AND ANALYSIS OF CONVEYING VIBRATOR

1) TEST RESONANT FREQUENCY OF VIBRATOR

During the experiment, in order to facilitate identification, the different partitions of piezoelectric ceramic chips of the piezoelectric vibrator are numbered as A, B, C, and D respectively. Zone A and B are ceramic chips partitions corresponding to the B_{11} order bending mode of the piezoelectric vibrator. If the ceramic chips in Zone A or Zone B are excited separately, the B_{11} order standing wave bending mode of the piezoelectric vibrator will be excited; Zone C and Zone D are the ceramic chips zones corresponding to the B_{15} order bending mode of the piezoelectric vibrator. If the ceramic chips in Zone C or Zone D are excited separately, the B_{15} order standing wave bending mode of the vibrator will be excited.

During the test, the excitation peak voltage is 80 V. Set the frequency to the value of the modal analysis result, and measure the resonant frequency of each group of piezoelectric ceramic chips as shown in Table 1.

It can be seen from the table that after the vibrator is installed on the base, the two frequencies of the same bending mode of the vibrator are equal.

2) MODAL TEST OF VIBRATOR IN RESONANT STATE

When testing the amplitude distribution of the particle on the surface of the vibrator under the resonant state, in order to make the test results as accurate as possible, 181 test points were selected on the entire circumference of the ring vibrator, with a distance of 2° between each point. The position of the initial teeth for testing remained unchanged, so that each test point is on the tooth surface. The amplitude distribution of some particles on the surface of the vibrator under the B_{11} bending mode (the vibrator installed before the base) excited by group A and group B is tested respectively. As shown in Figure 15 (Figure 16).

The piezoelectric ceramic chips of group A and group B (group C and group D) of the vibrator are respectively excited by a sine signal with the frequency of 24.69 kHz (39.31 kHz). The peak value of the excitation voltage is 80 V. The amplitude distribution of the particle on the surface of the vibrator is measured as shown in Figure 15 (Figure 16) (the test points are the same for each test). The solid line in the figure is

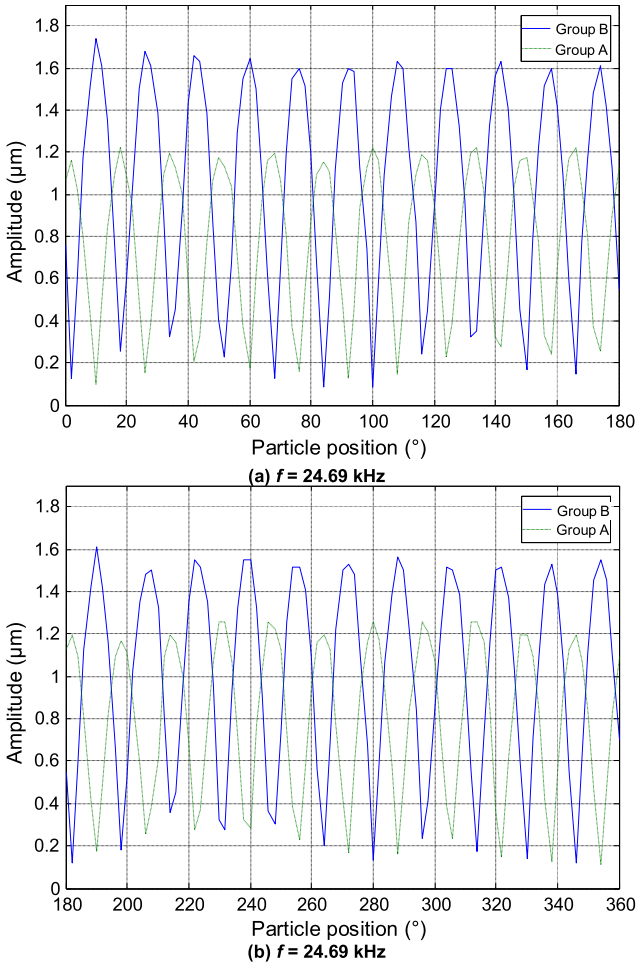

FIGURE 15. Amplitude distribution of the vibrator's B_{11} vibration mode.

the amplitude distribution of the particle when the piezoelectric ceramic chips of group B (C) are excited, The dotted line is the amplitude distribution of particles when group A (D) piezoelectric ceramic chips are excited.

As shown in Figure 15 and Figure 16 that the distribution laws of the solid line and the dotted line are almost the same, and there is a phase difference between the two, which is caused by the difference of 1/4 wavelength between the two groups of piezoelectric ceramic chips. The peak point of one mode of the two curves is the zero point of the other mode. It can be seen that the two bending modes of the same order of the vibrator measured actually conform to the characteristics of orthogonality at the same frequency. The two curves shown in Figure 15 have obviously different amplitudes of extreme points, which is due to the difference in the performance of the two groups of piezoelectric ceramic chips.

B. ANALYSIS OF AMPLITUDE CHARACTERISTIC OF THE CONVEYING VIBRATOR

1) RELATION BETWEEN DRIVING VOLTAGE AND AMPLITUDE

The relationship between the driving voltage and the amplitude distribution of the particle on the vibrator's surface

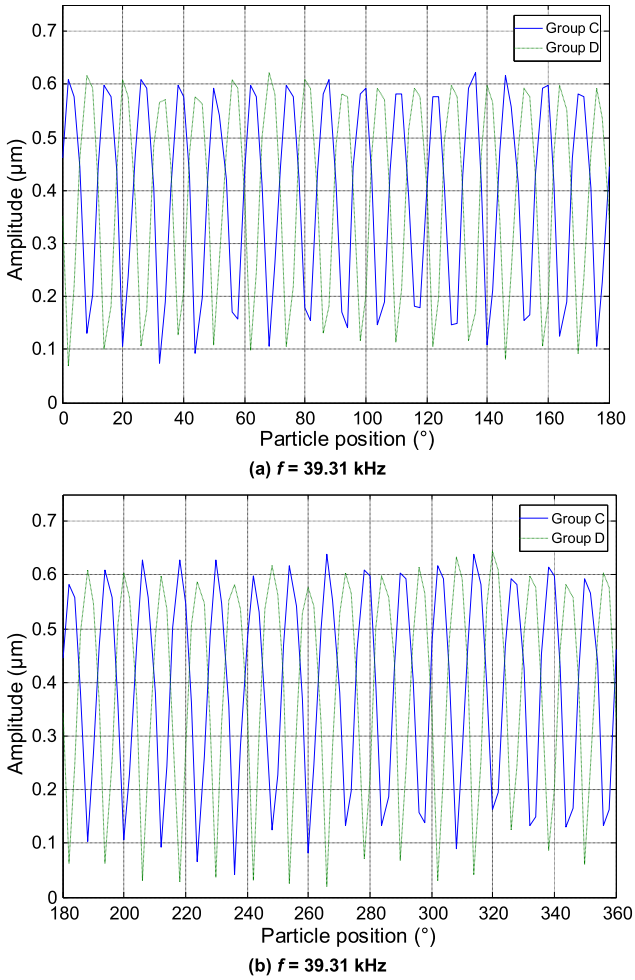

FIGURE 16. Amplitude distribution of the vibrator's B_{15} vibration mode.

is tested when other conditions remain fixed. Taking the B_{15} order bending mode of the vibrator as an example, the sinusoidal signal with the frequency of 39.31 kHz is used to excite group D piezoelectric ceramic chips of the vibrator, so that the driving voltage varies in the range of 30 V-200 V, with the increment is 10 V. The relationship between the vibration amplitude of a particle on the vibrator's surface and the driving voltage is measured as shown in Figure 17. The curve in the figure shows that the amplitude increases linearly with the increase of the driving voltage when the working frequency remains constant.

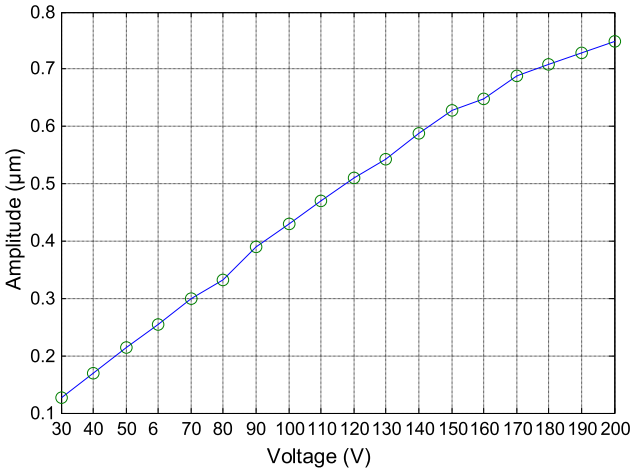

FIGURE 17. The relational curve between amplitude and voltage.

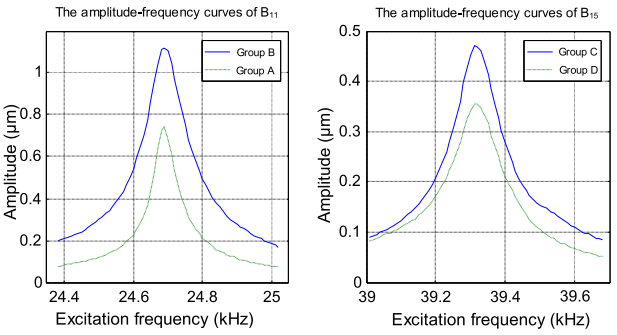

FIGURE 18. The amplitude-versus-frequency curves of the vibrator.

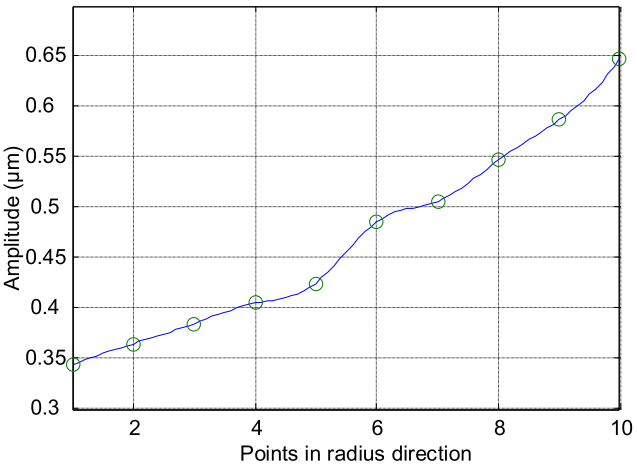

FIGURE 19. The amplitude distribution of the radical points.

2) RELATION BETWEEN OPERATING FREQUENCY AND AMPLITUDE

When the excitation voltage is fixed, adjust the frequency of the input signal to make the excitation frequency of the vibrator change near the resonant frequency. The adjustment step is 10 Hz. Test the change curve of particle amplitude on the vibrator's surface with the frequency. The test results are shown in Figure 18.

3) RADIAL PARTICLE AMPLITUDE DISTRIBUTION

The width of the ring vibrator is selected as 10 mm, and a test point is selected every 1 mm in the width direction, starting from the point closest to the center of the circle. The test points are numbered from 1 to 10. The amplitude distribution of the 10 selected test points is tested experimentally by using the sinusoidal signal with the driving voltage of 80 V, and

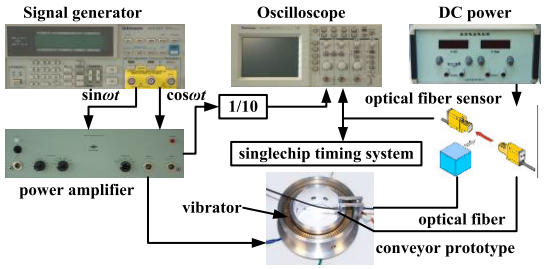

FIGURE 20. The schematic diagram of the experimental device for conveyor performance test.

the excitation frequency of 39.31 kHz to excite the C group piezoelectric ceramic chips of the vibrator. The test results are shown in Figure 19.

It can be seen from the curve that under the cylindrical coordinate θ, the amplitude of coordinate particle increases with the increase of polar coordinate r. The experimental results are consistent with the theoretical analysis results.

IV. CONVEYING PERFORMANCE TEST

The performance test of the conveying speed is carried out with the experimental prototype, and according to the test results, the influence rules of the main factors such as amplitude, working frequency and material type on the conveying speed are analyzed and discussed.

A. SCHEME OF EXPERIMENTAL TEST

The conveying capacity of ultrasonic material conveying device is affected by many factors, ignoring secondary environmental factors such as temperature and humidity [20]. This paper only examines the impact of several major factors, such as amplitude, working frequency, material type, etc. Experimental materials: brass cylinder, aluminum cylinder, steel tapered roller, stainless steel block, plastic block, nut, bearing, bolt, screw, tablet, grain, etc. The schematic diagram of the experimental device for conveyor performance test is shown in Figure 20.The optical fiber sensor is used to test the conveying performance of the conveying device. When the material passes through the transmitter and receiver of the sensor, the sensor integrates the detected signal and outputs a response signal. The digital oscilloscope connected to the sensor is used to display the response signal, observe and record the information of the response signal (including signal frequency, period, amplitude, etc.), At the same time, the response signal of the sensor is output to the self-made microcontroller timing system to display the time used by the material movement, and then the movement rate of the material is calculated.

B. ANALYSIS OF EXPERIMENTAL RESULTS

1) RELATION BETWEEN AMPLITUDE AND CONVEYING SPEED

Because the change rule and trend of the conveying speed between the B_{11} mode and B_{15} mode of the vibrator are identical, only the amplitude is slightly different, but also the change of the corresponding fixed ratio; Therefore, this paper only take the B_{15} order working modes of the vibrator as an example, the relationship between the particle amplitude on the surface of the vibrator and the conveying speed is analyzed. Adjust the frequency of the input alternating signal to 39.31 kHz, so that the conveying system is in resonance state. Adjust the input signal voltage in increment of 0.1 μm. Make the displacement of particle on the vibrator's surface change from 0.2 μm to 1.1 μm. The variation curve of the speed of the conveying tapered roller with the amplitude is obtained, as shown in Fig. 21.

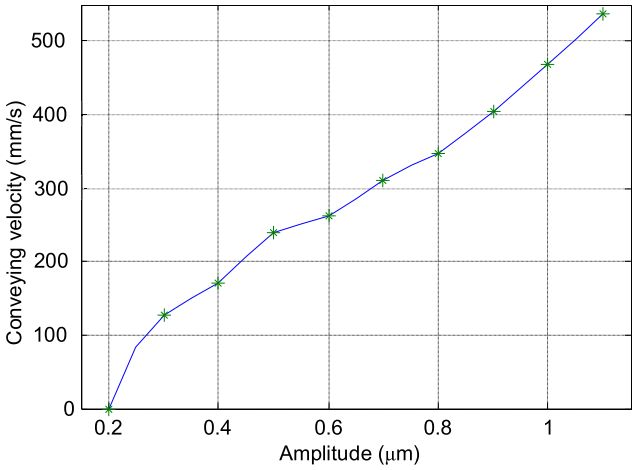

FIGURE 21. Relationship between amplitude and conveying velocity.

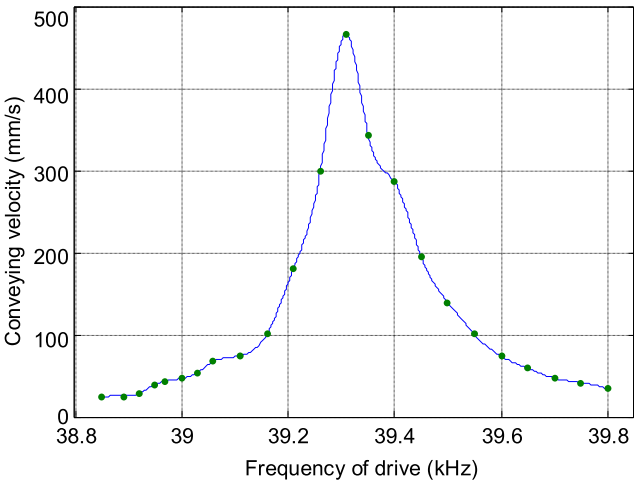

FIGURE 22. Relationship between driving frequencies and velocity.

It is found from Figure 21 that when the amplitude is less than 0.2 μm, the conveying device cannot transport materials well. When the amplitude exceeds 0.2μm, the conveying device starts to transport materials slowly. With the increase of amplitude, the conveying speed increases approximately linearly. When the amplitude of the particle on the vibrator's surface is 0.2 μm - 0.3 μm, the test piece transported by the vibrator rotates close to the inner ring of the conveyor's

base, indicating that the speed of the test piece is low and the centrifugal force is small, which is not enough to overcome the influence of the bending vibration amplitude outside the vibrator on the test piece. When the amplitude of particle on the vibrator's surface exceeds 0.3 μm, the delivered test piece rotates closely against the outer ring of the conveyor's base under the action of centrifugal force.

As shown in Figure 17 and Figure 21 that the amplitude of the particle on the vibrator's surface basically increases linearly with the increase of the driving voltage when the working frequency is kept constant, while the conveying speed of the conveying device also increases linearly with the increase of the amplitude. The conveying speed of the conveying device is increase with the increase of the driving voltage. When the input voltage is too low, the conveying device has almost no conveying capacity. Because the driving power is too small, it is not enough to generate enough amplitude to drive the material to move. With the increase of voltage, the amplitude of vibration generated is gradually increased; the conveying speed is also gradually increased. However, when the input voltage value is too high, the piezoelectric ceramic chips will overheat which shorten the service life of the ceramic chips and make the resonant frequency point of the conveyor drift.

TABLE 2. The results of the experiment.

	Contact area (mm2)	Time (s)	Speed (mm/s)
The large area is the contact surface	35.260	6.283	450.008
The small area is the contact surface	22.900	10.114	279.553

2) RELATION BETWEEN DRIVING FREQUENCY AND CONVEYING SPEED

Adjust the voltage of the input signal so that the maximum amplitude of the particle on the vibrator surface is 1 μm. The relationship between the running frequency of the conveying device and the conveying speed under the B_{15} order working mode of the vibrator is tested experimentally. Select a single tapered roller as the test material. When other conditions are fixed, adjust the frequency value of the input signal to test the conveying speed of the material at different working frequencies. The experimental results are shown in Figure 22.

The experimental device has good conveying performance in the range of 38.85 kHz-39.8 kHz, and the maximum conveying rate is about 39.31 kHz. It can be seen that the conveying speed of the conveying device can be adjusted by changing the working frequency. However, the conveying speed of the conveying device is very sensitive to the change of frequency. When the working frequency deviates too much from the resonant frequency, the conveying device cannot convey materials very well. Even if it can conveying materials slowly, the phenomenon that the test piece moves forward while rotating or even only rotates in place will occur. It can

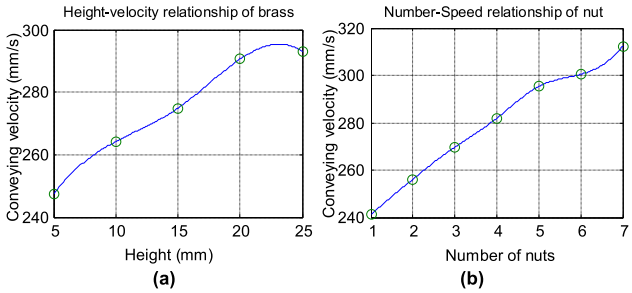

FIGURE 23. Relation curves between the quality and the feeding velocity.

be seen that the operating frequency has a great impact on the conveying performance of the ultrasonic material conveying device, and the system should work at its resonant frequency as far as possible.

3) RELATIONSHIP BETWEEN CONTACT AREA AND CONVEYING SPEED

Adjust the amplitude of the particle on the vibrator's surface to 1 μm under the B_{15} order working mode of the vibrator. Test the relationship between the conveying speed and the contact area of the test piece with the same mass (with the same material) under the resonant frequency. Take a single tapered roller as an example (the large area is φ 6.7mm, small area is φ 5.4mm, 10.8mm in height and 2.68g in weight), respectively test the running speed of the tapered roller with the large area as the contact surface and the small area as the contact surface. The experimental results are shown in Table 2.

It can be seen from Table 2 that for the same test piece, the contact area between it and the conveying vibrator is not equal, which will lead to the unequal speed of the test piece. The larger the contact area is, the more contact points and friction between the test piece and the conveying vibrator are, and the faster the test piece runs.

4) RELATION BETWEEN MATERIAL TYPE AND CONVEYING SPEED

Using the above method, adjust the power frequency to make the ultrasonic material conveying device in the resonant state, test several materials with different materials, densities, shapes and surface roughness, and analyze the test results.

The test results show that the ultrasonic material conveying device has certain selectivity for conveying objects: it has good conveying performance for materials with heavy weight and not very smooth surface, such as tapered roller, M5 hexagon nut, M5 cap nut, etc; For materials with the same quality but different surface roughness, their conveying conditions are different; It has good conveying performance for larger materials such as tablets and grains. It has conveying capacity for smaller materials such as red beans (0.1 g), M2 hexagon nuts, etc., but the materials will jump violently during the conveying process; For rubber materials with hard materials, such as tombarthite modified teflon

friction materials, it has a certain conveying capacity, but for soft rubber materials with smooth surfaces, the conveying capacity of the conveying device is poor, and there is almost no conveying capacity.

5) RELATIONSHIP BETWEEN QUALITY AND CONVEYING SPEED

Take two materials, brass cylinder and M5 hexagon nut, for example, to test the relationship between the mass of the test piece and the conveying speed when the contact area between the test piece and the conveying device remains unchanged (the bottom area of the test piece remains unchanged), and when the height of the test piece or the number of test pieces changes.

Under the same driving voltage and operating frequency, several brass cylinders (M5 hexagon nuts) are listed together, and the lowest test piece (base test piece) that directly contacts the conveying vibrator is kept unchanged. The relationship between the height change of brass test piece (variation range is 5 mm - 25 mm, the increment is 5 mm) and the conveying speed, and the relationship between the number of hexagon nuts (variation range is 1-7) and the conveying speed are tested respectively. The test results are shown in (a) and (b) in Figure 23.

It can be seen from Figure 23 that the conveying speed of the conveying device increases with the increase of material quality. The greater the mass of the material, the greater the contact pressure and contact deformation between the material and the conveying vibrator, the greater the friction between the conveying vibrator and the material, and the greater the conveying speed of the vibrator. The experimental results show that the conveyor can conveying materials well under different working modes; The conveying speed is very sensitive to the change of working frequency and reaches the maximum at the resonance point; The conveying speed of the conveying vibrator is linear with the amplitude.

Moreover, the piezoelectric vibration feeding device in the ultrasonic frequency domain moves smoothly and orderly with high efficiency due to its silent vibration feeding carrier and small amplitude, It has a very broad application prospect in the production fields requiring low noise and clean environment such as drug delivery and electronic components.

V. CONCLUSION

In this paper, ANSYS finite element analysis software is used to design the structure of the ring conveying vibrator, determine the structural size parameters of the vibrator, and optimize the B_{11}, B_{15} order bending modes and corresponding natural frequencies of the vibrator. A multi frequency design scheme with multiple bending modes for the same piezoelectric vibrator is realized by the design of the polarization of the piezoelectric ceramic chips in different zones. Based on the results of theoretical analysis, the principle prototype of a ring ultrasonic conveying device for material conveying performance experiment was designed and manufactured, and a series of experimental studies are carried out.

The amplitude distribution characteristics of particle on the vibrator's surface are tested experimentally. The experimental results show that the amplitude of the particle on the vibrator's surface increases linearly with the increase of the driving voltage when the excitation frequency is constant; When the driving voltage is constant, the particle amplitude reaches the maximum when the vibrator reaches resonance; The amplitude of particles on the same radius increases with the increase of polar coordinates.

The conveying performance of the conveyor under different working modes was tested experimentally. The test results show that the ultrasonic material conveying device has good conveying capacity under different working modes, can transport materials stably, and can be adjusted within a certain range; The conveying speed ratio corresponding to the B_{15}, B_{11} order working modes of the conveying device is a fixed value, and the experimental test results are consistent with the theoretical analysis values.

The conveying performance of the conveying device when conveying different materials is studied and the effects of excitation frequency, particle amplitude on the surface of the vibrator, material quality and contact area on the conveying speed are analyzed. The experimental results show that under the same driving conditions, the conveying device has a certain selectivity for the conveyed materials; The conveying speed is sensitive to the change of excitation frequency, and the conveying speed of the conveying device is the largest under the resonant state; The transport rate is proportional to the particle amplitude on the surface of the vibrator; When the contact area between the material and the conveying device is equal, the conveying speed increases linearly with the increase of material quality (number).

REFERENCES

[1] Y. He, Z. Yao, S. Dai, and B. Zhang, "Hybrid simulation for dynamic responses and performance estimation of linear ultrasonic motors," *Int. J. Mech. Sci.*, vols. 153–154, pp. 219–229, Apr. 2019.
[2] C. Jiang, X. Wu, D. Lu, Z. Xu, and L. Jin, "Contact modeling and performance evaluation of ring type traveling wave ultrasonic motors considering stator teeth," *Ultrasonics*, vol. 117, Dec. 2021, Art. no. 106518.
[3] Y. Deng, G. Zhao, X. Yi, and W. Xiao, "Contact modeling and input-voltage-region based parametric identification for speed control of a standing wave linear ultrasonic motor," *Sens. Actuators A, Phys.*, vol. 295, pp. 456–468, Aug. 2019.
[4] Y. Tanoue and T. Morita, "Opposing preloads type ultrasonic linear motor with quadruped stator," *Sens. Actuators A, Phys.*, vol. 301, Jan. 2020, Art. no. 111764.
[5] R. Niu, H. Zhu, and C. Zhao, "A four-legged linear ultrasonic motor: Design and experiments," *Rev. Sci. Instrum.*, vol. 91, no. 7, Jul. 2020, Art. no. 076107.
[6] S. Izuhara and T. Mashimo, "Characterization of bulk piezoelectric element-based ultrasonic motors," *ROBOMECH J.*, vol. 7, no. 1, p. 31, Aug. 2020.
[7] S. Miyake, T. Harada, H. Shimizu, S. Kishimoto, and T. Morita, "High-power characteristics of (Bi, Na) TiO_3-$BaTiO_3$ ceramics and application in miniature ultrasonic motor," *Sensors Mater.*, vol. 32, no. 7, pp. 2443–2452, Jul. 2020.
[8] R. Niu, J. Liu, H. Zhu, and C. Zhao, "Design and evaluation of a novel light arc-shaped ultrasonic motor," *AIP Adv.*, vol. 9, no. 6, Jun. 2019, Art. no. 065009.
[9] F. Wang, U. Nishizawa, H. Tanaka, and S. Toyama, "Development of miniature spherical ultrasonic motor using wire stators," *J. Vibroeng.*, vol. 20, no. 8, pp. 2939–2950, Dec. 2018.

[10] K. Miyoshi and T. Mashimo, "Miniature direct-drive two-link using a micro-flat ultrasonic motor," *Adv. Robot.*, vol. 32, no. 20, pp. 1102–1110, Sep. 2018.
[11] Y. Liu, S. Shi, C. Li, W. Chen, and J. Liu, "A novel standing wave linear piezoelectric actuator using the longitudinal-bending coupling mode," *Sens. Actuators A, Phys.*, vol. 251, pp. 119–125, Nov. 2016.
[12] M. Kucera, E. Wistrela, G. Pfusterschmied, V. Ruiz-Díez, T. Manzaneque, J. Hernando-García, J. L. Sánchez-Rojas, A. Jachimowicz, J. Schalko, A. Bittner, and U. Schmid, "Design-dependent performance of self-actuated and self-sensing piezoelectric-AlN cantilevers in liquid media oscillating in the fundamental in-plane bending mode," *Sens. Actuators B, Chem.*, vol. 200, pp. 235–244, Sep. 2014.
[13] W.-H. Lee, C.-Y. Kang, D.-S. Paik, B.-K. Ju, and S.-J. Yoon, "Butterfly-shaped ultra slim piezoelectric ultrasonic linear motor," *Sens. Actuators A, Phys.*, vol. 168, no. 1, pp. 127–130, Jul. 2011.
[14] Z. Li, Z. Wang, P. Guo, L. Zhao, and Q. Wang, "A ball-type multi-DOF ultrasonic motor with three embedded traveling wave stators," *Sens. Actuators A, Phys.*, vol. 313, Oct. 2020, Art. no. 112161.
[15] S. Borodinas, P. Vasiljev, D. Mazeika, R. Bareikis, and Y. Yang, "Design optimization of double ring rotary type ultrasonic motor," *Sens. Actuators A, Phys.*, vol. 293, pp. 160–166, Jul. 2019.
[16] S. L. Zhou and Z. Y. Yao, "Design and optimization of a modal-independent linear ultrasonic motor," *IEEE Trans. Ultrason., Ferroelect., Freq. Control*, vol. 61, no. 3, pp. 535–546, Mar. 2014.
[17] Z. Huang, S. Shi, W. Chen, L. Wang, L. Wu, and Y. Liu, "Development of a novel spherical stator multi-DOF ultrasonic motor using in-plane non-axisymmetric mode," *Mech. Syst. Signal Process.*, vol. 140, Jun. 2020, Art. no. 106658.
[18] X. Xin, Y. Yu, J. Wu, X. Gao, Z. Li, X. Yi, W. Chen, and S. Dong, "A ring-shaped linear ultrasonic motor based on PSN-PMS-PZT ceramic," *Sens. Actuators A, Phys.*, vol. 309, Jul. 2020, Art. no. 112036.
[19] D. Lu, Q. Lin, B. Chen, C. Jiang, and X. Hu, "A single-modal linear ultrasonic motor based on multi vibration modes of PZT ceramics," *Ultrasonics*, vol. 107, Sep. 2020, Art. no. 106158.
[20] S. Izuhara and T. Mashimo, "Design and characterization of a thin linear ultrasonic motor for miniature focus systems," *Sens. Actuators A, Phys.*, vol. 329, Oct. 2021, Art. no. 112797.

JIAN ZHANG received the B.S. and M.S. degrees in control theory and control engineering from the Liaoning University of Technology, China, in 2005 and 2008, respectively, and the Ph.D. degree in power electronics and power transmission from the Shenyang University of Technology, China, in 2022. He is currently a Professor with the School of Electrical Engineering, Yingkou Institute of Technology, China. His research interests include artificial intelligence and modern motion control, power electronics and power transmission, synchronous motor excitation system design and research, special motor design and control, design, and the control of ultrasonic motor.

XIAOZHU WANG received the B.S. and M.S. degrees in mechanical design and theory from the Liaoning University of Technology, China, in 2005 and 2008, respectively. She is currently an Associate Professor with the School of Mechanical and Power Engineering, Yingkou Institute of Technology, China. Her research interests include mechanical design and theory, ultrasonic piezoelectric technology and theory, design, and the control of ultrasonic motor.